INFLUENCE OF FLAPPING WING UNSTEADY MOTION ON AERODYNAMIC PERFORMANCE OF HORIZONTAL TAIL

Yin Yang, Dong Li
Northwestern Polytechnical University
yangyin059@live.cn;ldgh@nwpu.edu.cn

Keywords: *flapping wing; horizontal tail; pitching; plunging*

Abstract

For analyzing the aerodynamic performance of horizontal tail during the pitching and plunging motion of flapping wing, the flapping wing micro aerial vehicle (FMAV) ASN211, which is independently developed by Northwestern Polytechnical University, is utilized in this work as the object of investigation. The actual computational model is built by combining the flapping wing and horizontal tail of ASN211 in tandem in 2D space. In order to obtain the unsteady motion of the flapping wing, the dynamic mesh and User-Defined Function is applied in this study to control the mesh deformation and to define its periodic motion respectively. The final computational results, which are obtained by fluent, indicate that the aerodynamic force of horizontal tail has periodic variation just as that of the flapping wing; furthermore, the period of the variations is the same as the motion of flapping wing. The results also reveal that the drag and moment of horizontal tail agree very well with the force under steady state. The differences between the lift of the horizontal tail and the force under steady condition are induced by the tall on the horizontal tail.

1 Introduction

Flapping wing micro aerial vehicle (FMAV) is a category of flight vehicle that emulates the flight principles of a bird or insect. The design of FMAV involves a large number of integrant parts, such as Micro Electro Mechanical System (MEMS), aerodynamics, materials and etc. As the lift and thrust are provided by the dynamic surface and flex-wings, and the control moment [1] is given by control surface and tail, the key points of aerodynamic design is the design of flex-wings and tail. As it is difficult to install a flap on FMAV, tail becomes an important part of FMAV flight [2]. Tail provides controlling moment and static stability like that of an ordinary aircraft, however, it has more complicated dynamic performance produced by flapping wing on FMAV. Researchers of Northwestern Polytechnical University have done some experiments to analyze the tail of FMAV in the past years. These experiments have confirmed the significance of FMAV tail as they have shown that the tail has great impact on the stability, drag and aerodynamic center.

Researchers have done some experiments and numerical calculations to analysis the FMAV in different sides. However, until recently, most of the studies on FMAV are interested in the investigation of the flapping wing performance. Many authors have discussed the force on the flapping wing or its unsteady mechanism which will produce high lift [3] and thrust [4, 5] through experiments and numerical computations. Sun M [6], who announces the high lift mechanism of an insect, is such an example. Few researchers put their attention on the influence of the flapping-wing fluttering to the horizontal tail.

Studies on airfoil combination have shown that the wake [7-9] generated by a moving airfoil may have a great impact on the motion of the second airfoil. The wake interference may prevent or cause flow separation, suppress or promote aeroelastic fluttering, increase or

decrease flight performance. As a result, the wake generated by flapping wing will affect the horizontal tail aerodynamic performance, which will induce a performance that is quite different from that of the steady state. Considering the importance of horizontal tail for flight control and many other aspects, it is our belief that the analysis of the performance of the horizontal tail is an indispensable part of FMAV design.

2 Numerical Simulation Methods

2.1 Flow Solver

There are many approaches for the FMAV analysis, for instance, the unsteady panel method, the unsteady vortex lattice method, the unsteady Euler solver and Navier-Stokes solver. In this work, flow solver is performed by the unsteady Navier-Stokes solver, which is provided by the Computational Fluid Dynamics (CFD) software fluent.

The flow field here is assumed to be fully turbulent, and then the turbulence model SST $k-\omega$ is applied. Unsteady Navier-Stokes solver is used here to compute the viscous flow around the flapping stationary airfoil combination in tandem.

2.2 Mesh Generation and Motion Definition

2.2.1 Mesh

The computational model, which is a simplification of the 3D model of ASN211 in Fig. 1, is a combination of two airfoils in 2D space. The details of the simplified model are shown in Fig. 2.

Since the wing of ASN211 has a camber and the leading edge of which is supported by a pole, we should choose the airfoil that has similar camber and leading edge radian as that of the ASN211 in the modeling process. Consequently, birdlike airfoil e376 is selected. Because the tail of ASN211 is almost a flat plate, we choose NACA0002 as the trailing airfoil.

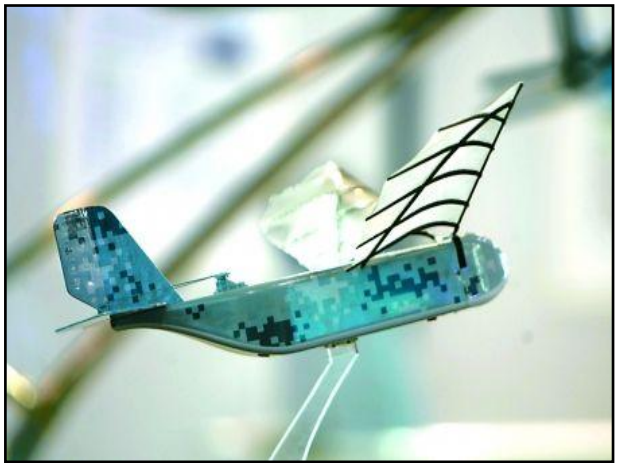

Fig. 1. Prototype of Plane.

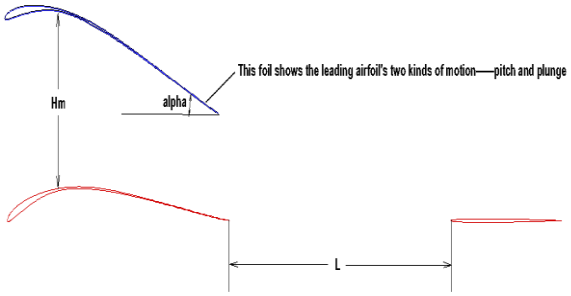

Fig. 2. Simplified Model.

Parameters are determined according to the original layout of ASN211. As shown in Fig. 2, the chord lengths of leading airfoil and trailing airfoil are 10 centimeters and 5 centimeters respectively. The distance between two airfoils, which is denoted by L in the figure, is 10 centimeters. The flapping frequency of the flapping wing (*f*) is 10 hz, and velocity of far field (V_∞) is 10m/s.

Unstructured mesh is applied in the unsteady computation for the reason that there may have large pitching and plunging amplitudes on the airfoils. The details of the mesh are shown in Fig. 3. For some MAVs, the pitching amplitude could reach up to 30 degrees and the plunge amplitude could be as much as a chord length of the flapping wing. In these conditions, large mesh deformation would be generated.

In order to achieve the control of mesh deformation, fluent provides us three different

choices. They are spring-based smoothing, dynamic layering and local remeshing. Because of the large mesh deformation and unstructured mesh, a combination of the spring-based smoothing and the local remeshing is used in this work, which finally turned out to be a very good combination.

Fig. 3. Model Mesh.

2.2.2 Motion Definition

To facilitate the computation, it is important to choose appropriate tools for an expedient and accurate definition of the periodic motion of the leading airfoil. The dynamic mesh technique is used here to solve large mesh deformation. And the User-Defined Function (UDF), which is provided by Fluent, is applied to set the pitching and plunging motions as

$$\alpha(t) = \alpha_m \sin(\omega t) \quad (1)$$

and

$$h(t) = h_m \sin(\omega t) \quad (2)$$

respectively. Where the circular frequency ω is defined by

$$\omega = 2\pi f \quad (3)$$

The pitching and plunging motions were performed along the sinusoidal wave around the quarter-chord axis of the airfoil.

For computing the lift, drag and moment, we choose horizontal tail chord length as the reference chord length and one horizontal tail chord as the reference area. By convention, we assume that the moment that raises the head of an aircraft is positive and the quarter chord of flapping wing is the center of moment.

3 Numerical Verification

3.1 Model and Computation Grid

Before the computation, we have to verify the method applied is useful and applicable for the unsteady flow under consideration. As numerical verification is the prerequisite of simulations, we will demonstrate the feasibility of our method through several examples.

Here, we choose an example in the paper of Ismail H [10] that is very similar to our calculation to verify our method. The combination of flapping airfoil and stationary airfoil in tandem is presented in Fig. 4, in which the Xshift is 1.0c (c is airfoil chord length), and Yshift is zero.

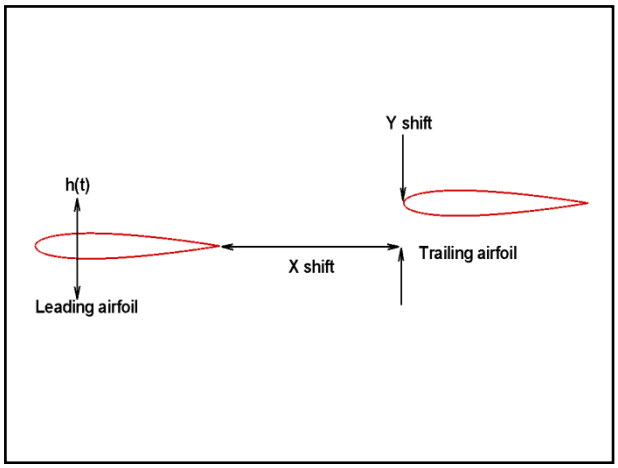

Fig. 4. Airfoil Combination in Tandem [10].

It is shown in Fig. 5 that Ismail H has applied the overlapping C-grids to discretize the computational domain. While in this work, we have used the unstructured mesh to achieve the discretization computational domain in this study, the details of which is presented in Fig. 6.

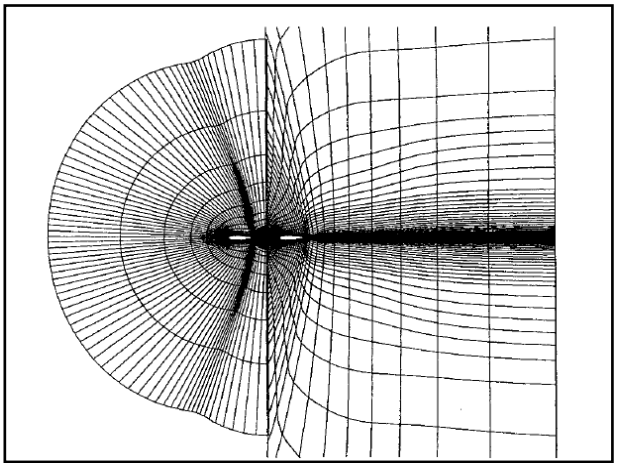

Fig. 5. Computational Domain with Overlapping C-grids in Reference [10].

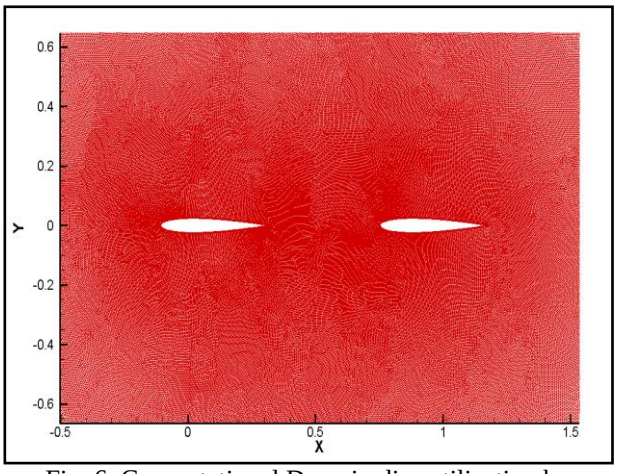

Fig. 6. Computational Domain discretilization by Unstructured Mesh.

3.2 Definition

In this case, the plunge motion of the leading airfoil is defined by

$$h = -A\cos(\omega t) \tag{4}$$

where A denotes the plunge amplitude, and ω is given by equation

$$k = \omega c / (2v_{\infty}) \tag{5}$$

The flow fields is computed in the condition that Ma=0.3 , Re_c=3.0×10^6 , $A = 0.1$c and $k = 1.5$.

3.3 Results

Time history of the lifts and drags on two airfoils are presented in Fig. 7 and Fig. 8 respectively. The lifts of the leading airfoil and trailing airfoil show great consistency with the results in the reference. It is also note worthy that the drags of both airfoils are not quite close to that of the reference. As we know, the computation of drags is always an aporia in computational fluid dynamics. The difference in numerical methods, meshing and many others are all possible factors that may cause deviations in computation. In this paper, we will pay our attentions on the variation trends of the drags rather than the exact values. So, the results obtained by fluent are fully acceptable.

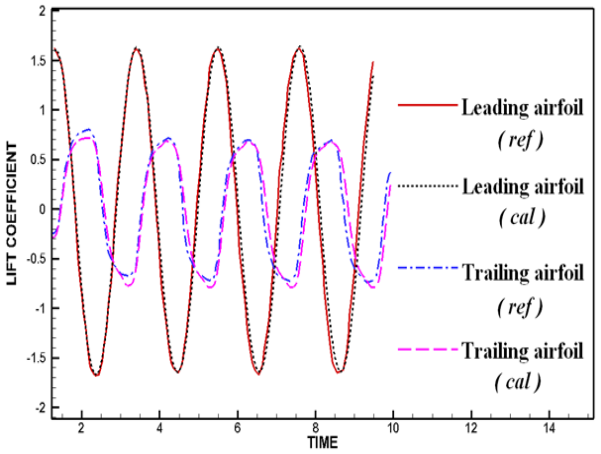

Fig. 7. Graphical Comparison of Lift Coefficients Obtained in This Study with the Lift in Reference [10].

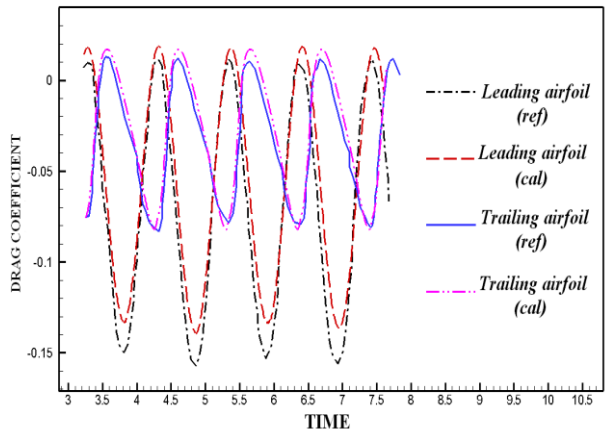

Fig. 8. Graphical Comparison of Drag Coefficients Obtained in This Study with the Drag in Reference [10].

4 Results and Discussion

The aerodynamic force of horizontal tail in unsteady state (flapping wing pitches or plunges) is predicted to be quite different from that of the steady state (flapping wing and horizontal tail keep static). Therefore, comparisons of the lifts,

drags and moments in two states will reflect the impact of the flapping wing motions on these aerodynamic forces.

4.1 Impact on Lift

It is shown in Fig. 9 that the maximum lift and stall angle of horizontal tail is 0.8 and 12.5 degrees respectively in steady state. When the flapping wing is doing pitching or plunging, we have received a higher maximum lift and stall angle, longer linear range of lift curve. The maximum lift coefficient reaches up to 1.1 and stall angle reaches up to 25 degrees during the unsteady motion of the flapping wing.

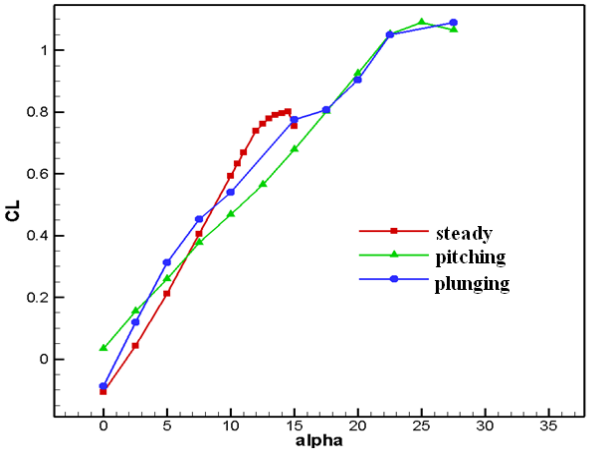

Fig. 9. Lift Curves of Horizontal Tail.

As shown in Fig. 10, the stall angle of flapping wing reaches up to 18 degrees which is much smaller than the horizontal tail stall angle in unsteady state. At some high angle of attack lower than the horizontal tail stall angle, horizontal tail is still effective after flapping wing time-averaged lift began to drop. This is meaningful for the maneuverability owing to the lift of horizontal tail offers nose- down moment to reduce the angle of attack to keep control failure away.

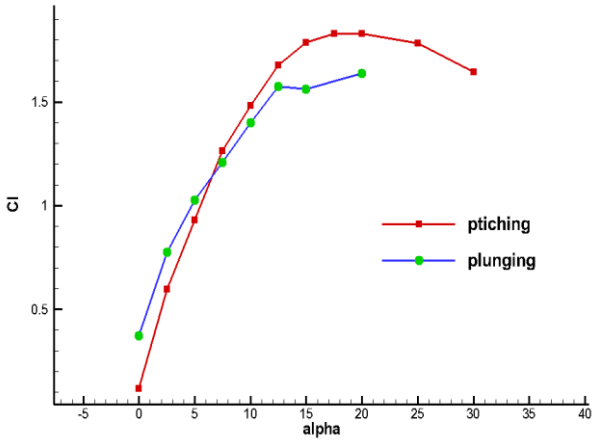

Fig. 10. Lift Curves of Flapping Wing.

The obtained dynamic lift coefficients are presented in Fig. 11 and Fig. 12. When the angle of attack(AOA) is 10 degrees, the Lift coefficient of horizontal tail achieves a periodic behavior with respect to the motion of the flapping wing. Furthermore, the periods of the lift coefficients of the tail resembles that of the flapping wing.

Horizontal tail lift oscillation caused by flapping wing gives rise to the structural vibration and noise level which is adverse to its invisibility. Lift oscillation also leads to the material fatigue, control surface deformation and manipulate failure even reversal. For these problems solving, appropriate horizontal tai shape, suitable flapping frequency and reasonable distribution benefit for the oscillation reduction, and dynamic lift coefficients supply a clue for the design consideration.

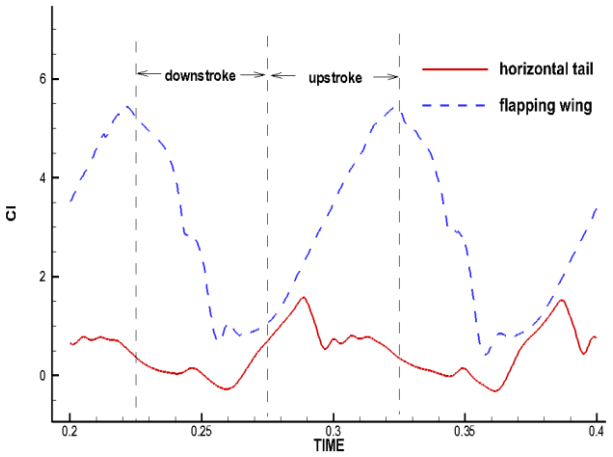

Fig. 11. Time History of Horizontal Tail and Flapping Wing Lift Coefficients When pitching, AOA=10°.

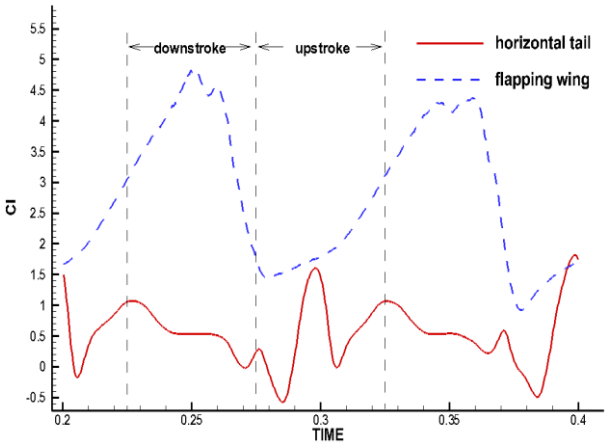

Fig. 12. Time History of Horizontal Tail and Flapping Wing Lift Coefficients When plunging, AOA=10° .

The maximum lift on horizontal tail appears as the flapping wing passes the dead position downward. Comparing to the lift on flapping wing, the lift on the tail has obvious phase.

For explaining the stall of horizontal tail in detail, we have done some research on the unsteady flow field. The reduced frequency is 0.3 too small to form the thrust produces vortex street. The velocity profile, which is presented in Fig. 13, is a drag profile that measured at 1.25c down-stream on the trailing edge of the flapping wing.

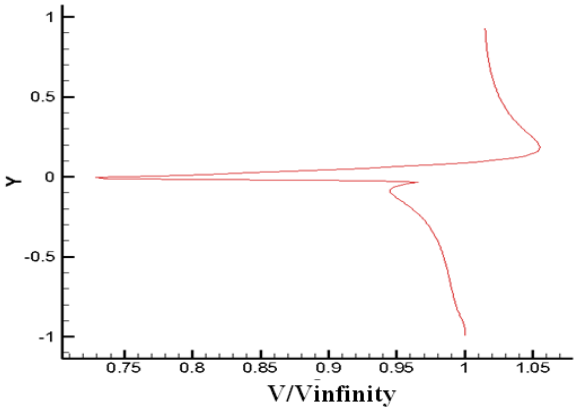

Fig. 13. Velocity Profile AOA=10° .

Therefore, because of the wake deflection caused by the angle of attack, there is a horizontal component for the time-averaged wake which is opposite to the flow direction and reduces the velocity in front of the horizontal tail. In the same fashion, there exists a vertical direction component that decreases the angle of attack of horizontal tail. These two reasons would delay the stall of horizontal tail.

4.2 Impact on Drag

As shown in Fig. 14, the drag coefficient of horizontal tail in steady state agrees well with the drag coefficient in unsteady state. This provides us information that predicts the time-averaged drag coefficient when the flapping wing is pitching or plunging by the drag coefficient in steady state. This approximation would save computation time and alleviate the computation complexity.

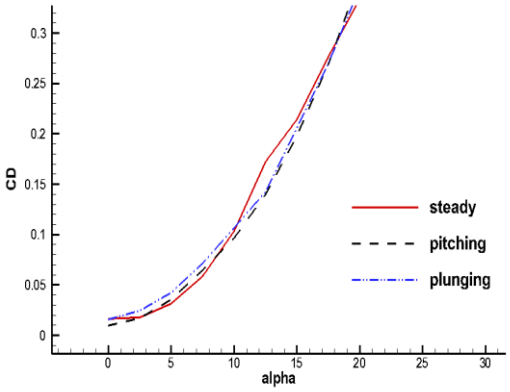

Fig. 14. Drag Curves of Horizontal Tail.

It is presented in Fig. 15 and Fig. 16 that the drag coefficients of horizontal tail attain a periodic behavior with respect to the flapping motion and its periods is similar to the flapping wing either. When the angle of attack is 10° , the drag coefficients of flapping wing and horizontal tail in steady state are 0.08312 and 0.1033 respectively . However, according to Fig. 15 and Fig. 16, the drag coefficient of flapping wing is much higher than 0.08312 most of the time, while the drag coefficient of horizontal tail appears to be much stable.

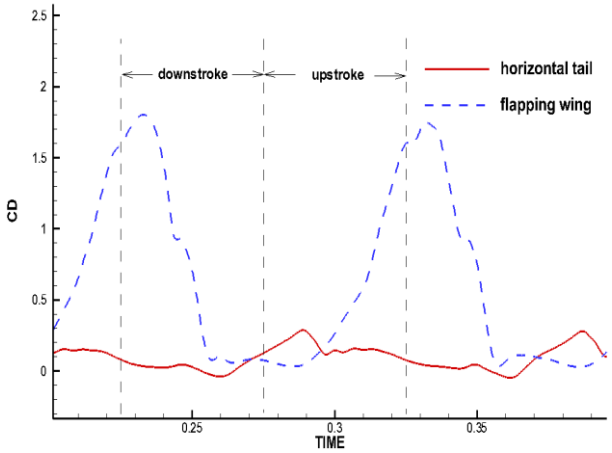

Fig. 15. Time History of Horizontal Tail and Flapping Wing Drag Coefficients When Pitching, AOA=10°.

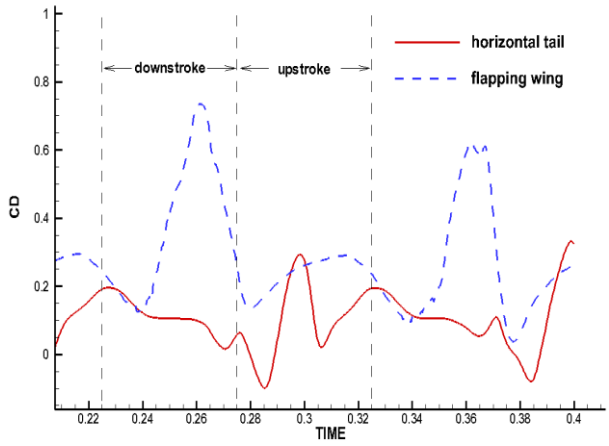

Fig. 16. Time History of Horizontal Tail and Flapping Wing Drag Coefficients When Plunging, AOA=10°.

4.3 Impact on Moment

In Fig. 17, the moment coefficients of horizontal tail indicate that there are only a few differences between steady moment and unsteady moment. But along with the unsteady motion of flapping wing, the moment coefficient of horizontal tail oscillates severely with time. Due to its long arm of force, the moment of horizontal tail is greater than the flapping wing moment.

Moment coefficient of horizontal tail also attains a periodic behavior with respect to the flapping motion and its cycle is the same as the flapping wing too, no matter with the motion type, see Fig. 18 and Fig. 19.

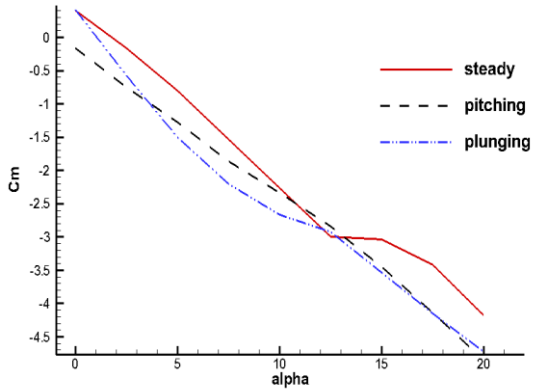

Fig. 17. Moment Curves of Horizontal Tail.

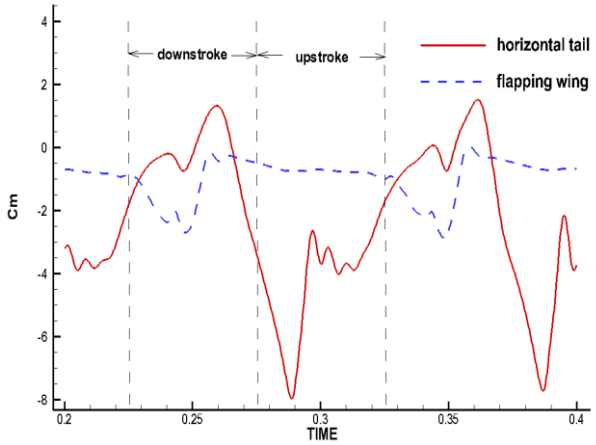

Fig. 18. Time History of Horizontal Tail and Flapping Wing Moment Coefficients WhenPitching, AOA=10°.

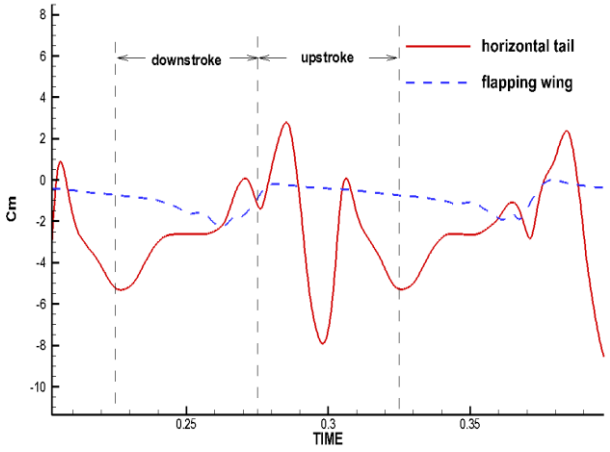

Fig. 19. Time History of Horizontal Tail and Flapping Wing Moment Coefficients When Plunging, AOA=10°.

5 Conclusion

Analysis on Horizontal tail of 2D airfoils combination simplified from 3D FMAV is based on Navier-Stokes solver, which is

provided by fluent used to compute unsteady flowfield about oscillatory pitching and plunge airfoils. Unsteady flowfield simulation has much confidence in fluent by means of the numerical verification. With the dynamic mesh technology application, controlling of mesh deformation offers high mesh quality for unsteady simulation.

In conclusion, the unsteady motion of flapping wing would induce a periodic behavior of the aerodynamic forces on horizontal tail. The periods of the forces variations are similar with the periods of the flapping-wing motion. Time-averaged drag and moment coefficients of horizontal tail have a little difference with the corresponding coefficients in steady state. Which indicate that the unsteady motion flapping wing has a great impact on the lift of horizontal tail.

References

[1] G.Sachs. What can be learned from unique lateral-directional dynamics properties of birds for mini-aircraft. *AIAA Atmospheric Flight Mechanics Conference and Exhibit*, hilton head south carolina, AIAA-2007-6311, pp 1-16, 2007.

[2] Kenneth H. Goodrich, Paul C. Schutte and Ralph A. Williams. Haptic-multimodal flight control system update. *11th AIAA Aviation Technology, Integration, and Operations Conference*, virginia beach, virginia, AIAA-2011-6984, pp 1-17, 2011.

[3] Ellington C P, Van den Berg C and Willmott A P, et al. Leading-edge vortices in insect flight. *Nature*, Vol. 384, pp 626-630, 1996.

[4] Freymuth P. Thrust generation by an airfoil in hover modes. *Experiments in Fluids*, Vol. 9, pp 17-24, 1990.

[5] K. D. Jones and M. F. Platzer. Numerical computation of flapping-wing propulsion and power extraction. *35th Aerospace Sciences Meeting and Exhibit*, reno navada, AIAA-1997-0826, pp 1-16, 1997.

[6] Sun M and Hossein H. Force and flow structures of an airfoil performing some unsteady motions at small Reynolds number. *Acta Aerodynamica Sinica*, Vol. 18, pp 96-102, 2000.

[7] Lucas Clemons, Hirofumi Igarashi and Hui Hu. An experimental study of unsteady vortex structures in the wake of a piezoelectric flapping wing. 48th *AIAA Aerospace Science Meeting Including the New Horizons Forum and Aerospace Exposition*, oriando florida, AIAA-2010-1025, pp 1-12, 2010.

[8] Fuchiwaki, M and Tanaka, K. Two-dimensional structure of the wake behind a pitchinging airfoil with higher non-dimensional pitchinging rate. J*ournal of visualization*, Vol. 4, No. 4, pp 323-329, 2001.

[9] Yu M L, Hu H and Wang Z J. Experimental and numerical investigations on the asymmetric wake vortex structures around an oscillating Airfoil. *50th AIAA Aerospace Sciences Meeting including the New Horizons Forum and Aerospace Exposition*, Nashville Tennessee, AIAA-2012-299, pp 1-20, 2012.

[10] Ismail H. Tuncer and Max F. Platzer. Thrust generation due to airfoil flapping. *AIAA Journal*, vol. 34, No. 2, pp 324-331, 1996.

Copyright Statement